CHAPTER

# 10

# Climate Sensitivity and Feedback Mechanisms

## 10.1 FOOLS' EXPERIMENTS[1]

Understanding and forecasting of climate change presents a great challenge to geoscientists. The surface climate of Earth is determined by a complex set of interactions among the atmosphere, the ocean, and the land, and these interactions involve physical, chemical, and biological processes. Many of these interactions are poorly understood, and important interactions and processes have probably yet to be discovered. Because it is apparent that humans have the capability to alter climate, it is necessary that we attempt to understand how the climate system works and make quantitative estimates of how our past, present, and future actions will change it. To make progress on a problem with the intimidating complexity of climate change, the proper response of a scientist is to begin by considering simpler questions and then add complexity as understanding is gained. The lessons drawn from these simple models must be taken seriously, but with the full realization that they may not be a faithful representation of nature.

In climate modeling, complexity is determined by the number and kind of processes or interactions among system components that are included. Once a starting point is chosen, one must decide in what order to bring additional processes or interactions into consideration, and with how much detail it is necessary to represent these processes. These decisions can be made on the basis of how important the processes are for the maintenance of climate, or on the basis of their importance for determining the magnitude or structure of a climate change response to a climate forcing of a given measure. The relationship between the measure of forcing and the magnitude of the climate change response defines what we will call the *climate sensitivity*. A process that changes the sensitivity of the climate

[1]"I love fools' experiments. I am always making them." —***Charles R. Darwin***

**Global Physical Climatology.** http://dx.doi.org/10.1016/B978-0-12-328531-7.00010-4

response is called a *feedback mechanism*. The strength of a feedback can also be quantified, and will be termed a *positive feedback* if the process increases the magnitude of the response, and *negative* if the feedback reduces the magnitude of the response. To construct a model of climate change, it is logical to order the feedback processes according to importance, and then include the most important feedbacks first. If positive and negative feedbacks of similar strength are possible, then it is important to include both simultaneously, or otherwise a very inaccurate estimate of the overall system sensitivity can be obtained.

For this discussion, it is useful to review the terms climate forcing and climate feedback. Climate forcing is a change to the climate system that can be expected to change the climate. Examples would be doubling the $CO_2$, increasing the total solar irradiance (TSI) by 2%, introducing volcanic aerosols into the stratosphere, etc. Climate forcings are usually quantified in terms of how many W $m^{-2}$ they change the energy balance when imposed. For example, instantaneously doubling the $CO_2$ changes the energy balance at the top of the atmosphere by about 4 W $m^{-2}$. A feedback process is a response of the climate system to surface warming that then alters the energy balance in such a way as to change the temperature response to the forcing. A positive feedback makes the forced response bigger, and a negative feedback makes it smaller. Classic examples of positive feedbacks are ice-albedo feedback and water-vapor feedback. When it warms, ice melts, and this reduces Earth's albedo and causes further warming. When it cools, ice grows, and this increases Earth's albedo, causing further cooling. In water-vapor feedback the saturation vapor pressure is very sensitive to temperature and water vapor is the most important greenhouse gas, producing the strongest positive feedback. The biggest negative feedback is Planck feedback. When the air gets warm, its radiative emission increases following Planck's Law. As the Earth gets warm, it emits more radiation, which cools more strongly.

## 10.2 OBJECTIVE MEASURES OF CLIMATE SENSITIVITY AND FEEDBACK

The concept of sensitivity can be used to judge which climate processes should be considered first and which can be neglected until later. Sensitivity can also be used as an objective measure of the performance of a model. Quantitatively, sensitivity is the amount by which an objective measure of climate changes when one of the assumed independent variables controlling the climate is varied. For example, we might ask how much the global mean surface temperature, $T_s$, changes if we vary the TSI, $S_0$; however, the global mean temperature is a function of more than the TSI. Suppose it depends on a number of variables $y_j$, which are all parametrically related to $S_0$, $y_j = y_j(S_0)$. Secondary variables would be temperature, water vapor,

other greenhouse gases, cloudiness, ice cover, land vegetation, and many others. Then the chain rule yields,

$$\frac{dT_s}{dS_0} = \frac{\partial T_s}{\partial S_0} + \sum_{j=1}^{N} \frac{\partial T_s}{\partial y_j} \frac{dy_j}{dS_0} \tag{10.1}$$

where partial and total derivatives are denoted by $\partial$ and $d$, respectively, and $N$ is the number of important subsidiary variables. The total change of surface temperature with respect to TSI is the sum of many contributions each made up of the partial derivative of surface temperature with respect to a secondary variable that controls surface temperature, times the total change of that secondary variable with respect to the TSI. As an example, if we increase the TSI, the specific humidity of air will increase because of the dependence of saturation vapor pressure on temperature. The increase of atmospheric water vapor will in turn lead to an increase in surface temperature, because of the greenhouse effect of the added water vapor.

We may simplify the concept of climate sensitivity somewhat by supposing that some *climate forcing*, $dQ$, with units of W m$^{-2}$ is applied to the climate system, and ask how it is related to a measure of climate change such as the change in global mean surface temperature, $dT_s$. We define the ratio of the climate response to the climate forcing as one measure of climate sensitivity.

$$\frac{dT_s}{dQ} = \lambda_R \tag{10.2}$$

As an example, we can consider the global mean energy balance at the top of the atmosphere.

$$R_{TOA} = \frac{S_0}{4}(1-\alpha_p) - F^{\uparrow}(\infty) = 0 \tag{10.3}$$

If we imagine that some forcing $dQ$ of the energy balance is applied, so that the climate is driven to some new equilibrium state with a new global mean surface temperature, then we can use the chain rule to write

$$\frac{dR_{TOA}}{dQ} = \frac{\partial R_{TOA}}{\partial Q} + \frac{\partial R_{TOA}}{\partial T_s}\frac{dT_s}{dQ} = 0 \tag{10.4}$$

from which, using (10.3) we obtain

$$\frac{dT_s}{dQ} = -\left(\frac{\partial R_{TOA}}{\partial T_s}\right)^{-1} = \left(\frac{S_0}{4}\frac{\partial \alpha_p}{\partial T_s} + \frac{\partial F^{\uparrow}(\infty)}{\partial T_s}\right)^{-1} = \lambda_R \tag{10.5}$$

In this simple model, the climate sensitivity is controlled by two basic feedback processes: One feedback is measured by the dependence of the

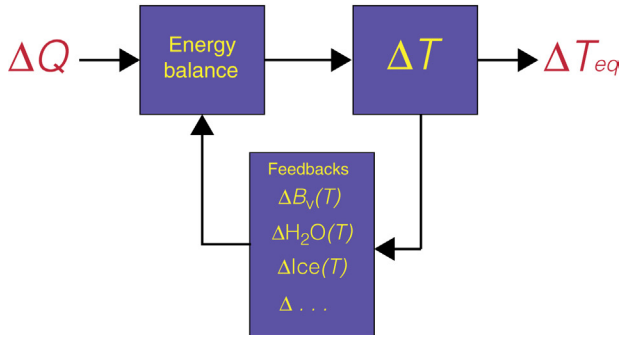


**FIGURE 10.1 Schematic diagram indicating the nature of a feedback process.** An initial climate forcing $\Delta Q$ changes the energy balance and leads to an initial temperature change $\Delta T$. This temperature change causes other changes in the climate system; a change in the Planck emission of terrestrial radiation $\Delta B_\nu(T)$, a change in the water vapor content $\Delta H_2O(T)$, a change in the ice coverage $\Delta \mathrm{Ice}(T)$, or some other change $\Delta\cdots$. These changes in turn then influence the energy balance leading to a further change in the temperature. When the temperature change is such that the feedbacks balance the forcing, then the system is in a new equilibrium with a temperature change $\Delta T_{eq}$.

emitted terrestrial radiation flux on surface temperature, and the other is measured by the dependence of the albedo on surface temperature. If the sensitivity parameter $\lambda_R$ is known, then we can estimate the global mean surface temperature change $dT_s$ expected from a given climate forcing $dQ$.

$$dT_s = \lambda_R \, dQ \tag{10.6}$$

Figure 10.1 illustrates the basic concept of a feedback process and distinguishes it from climate forcing. Once the climate forcing, $\Delta Q$, causes some initial temperature change, $\Delta T$, elements of the climate system respond to this temperature change. If the climate forcing is positive, then the temperature change is positive, the emission of terrestrial radiation increases following Planck's law $\Delta B_\nu(T)$, which acts to increase the radiative cooling of the climate, a negative feedback. Positive feedbacks result because water vapor increases with temperature, $\Delta H_2O(T)$, and ice cover decreases with temperature, $\Delta \mathrm{Ice}(T)$. When all the feedbacks are balanced and the system is in energy balance, then a new equilibrium temperature has been established, which is different by the amount $\Delta T_{eq}$.

## 10.3 BASIC RADIATIVE FEEDBACK PROCESSES

### 10.3.1 Planck Feedback

We may use the simple global mean model of Chapter 2 to evaluate the strength of the negative feedback associated with the temperature

dependence of thermal emission following Planck's Law (3.7). This may be the most important negative feedback controlling the surface temperature of Earth. The emission temperature of a planet is defined by the balance described by (10.3) with the outgoing terrestrial energy emission determined by the Stefan–Boltzmann Law, $F^{\uparrow}(\infty) = \sigma T_e^4$. If we ignore the dependence of albedo on temperature for the moment and assume that the surface temperature and the emission temperature are linearly related, then the sensitivity parameter for this model, which cools like a blackbody, is given by

$$(\lambda_R)_{BB} = \left( \frac{\partial(\sigma T_e^4)}{\partial T_s} \right)^{-1} = (4\sigma T_e^3)^{-1} = 0.26 \text{ K } (\text{W m}^{-2})^{-1} \tag{10.7}$$

The estimate of sensitivity obtained here indicates that about one-quarter of 1°C change in temperature will result from a 1 W $m^{-2}$ forcing of the energy balance. A 1 W $m^{-2}$ forcing of the energy balance can be produced by about a 5.7 W $m^{-2}$ change in the TSI, if the albedo is 0.3. If only Planck feedback is considered, it will take about a 22 W $m^{-2}$ or 1.6% change in TSI to produce a 1°C change in Earth's surface temperature. With such a stable climate, it would be difficult to produce the climate changes observed in the past, so we conclude that some strong positive feedback processes must also operate.

From radiative transfer model calculations, we can estimate that if we double the $CO_2$ concentration from 300 to 600 ppmv, and leave the temperature and humidity distributions as they are, then the outgoing longwave radiation (OLR) would decrease by about 4 W $m^{-2}$, which would result in an increase of the net radiation at the top of the atmosphere by the same amount. This is equivalent to a TSI increase of 1.67%, assuming a fixed albedo of 0.3. We can use (10.7) in (10.6) to estimate that about a 1°C global mean surface temperature increase would result from such a climate forcing.

### 10.3.2 Water Vapor Feedback

One of the most powerful positive feedbacks is associated with the temperature dependence of the saturation vapor pressure of water. As the temperature increases, the amount of water vapor in saturated air increases. Since water vapor is the principal greenhouse gas, increasing water vapor content will increase the greenhouse effect of the atmosphere and raise the surface temperature even further. Thus, the dependence of atmospheric water vapor on temperature constitutes a positive feedback.

Because much of Earth's surface is wet, the humidity of air near the surface tends to remain close to the saturation vapor pressure of air in contact

with liquid water. The temperature dependence of the saturation vapor pressure can be obtained from the Clausius–Clapeyron relationship,

$$\frac{de_s}{dT} = \frac{L}{T(\alpha_v - \alpha_l)} \tag{10.8}$$

where $e_s$ is the saturation vapor pressure above a liquid surface, $L$ is the latent heat of vaporization, $T$ is the temperature, $\alpha_v$ is the specific volume of the vapor phase, and $\alpha_l$ is the specific volume of the liquid phase. From (10.8) we can show that the change in saturation specific humidity divided by the actual value of specific humidity is related to the change in temperature divided by the actual temperature.

$$\frac{dq^*}{q^*} = \frac{de_s}{e_s} = \left(\frac{L}{R_v T}\right)\frac{dT}{T} \tag{10.9}$$

For terrestrial conditions $(L/R_vT) \approx 20$, so that a 1% change in temperature, which is about 3°C, is associated with about a 20% change in saturation specific humidity, or a 1 K change in temperature corresponds to a 7% change in saturation specific humidity.

It is observed that the relative humidity of the atmosphere, which is the ratio of the actual to the saturation humidity, tends to remain constant, even when the air temperature goes through large seasonal variations in middle to high latitudes. This is not too surprising, since we know that the relative humidity cannot exceed 100% for long and vapor is extracted very efficiently from the ocean when the relative humidity of air is low. As an estimate of the effect of water-vapor feedback on climate sensitivity, we may utilize a one-dimensional radiative-convective equilibrium model (see Section 3.10) in which we assume that the relative humidity remains fixed at observed values while the temperature changes. In this case, we find that the terrestrial radiation emitted from the planet increases much less rapidly with temperature than would be indicated by the Stefan–Boltzmann relationship. Moreover, the terrestrial emission increases linearly with surface temperature, rather than as the fourth power of temperature (Manabe and Wetherald, 1967).

Figure 10.2 shows the surface temperature obtained from a one-dimensional radiative-convective equilibrium model as functions of TSI and atmospheric $CO_2$ concentration, with two curves showing the result if specific humidity or relative humidity is fixed. In each case, the surface temperature changes faster with the forcing parameter when the relative humidity is fixed rather than specific humidity. In the case of fixed relative humidity (FRH), the water vapor increases about 7% for each degree of warming, so that a strong positive water-vapor feedback is present. The surface temperature increases approximately linearly with TSI, except in the case of fixed relatively humidity for which TSI greater than about 1.1 times today's gives a runaway greenhouse effect in this model. For $CO_2$

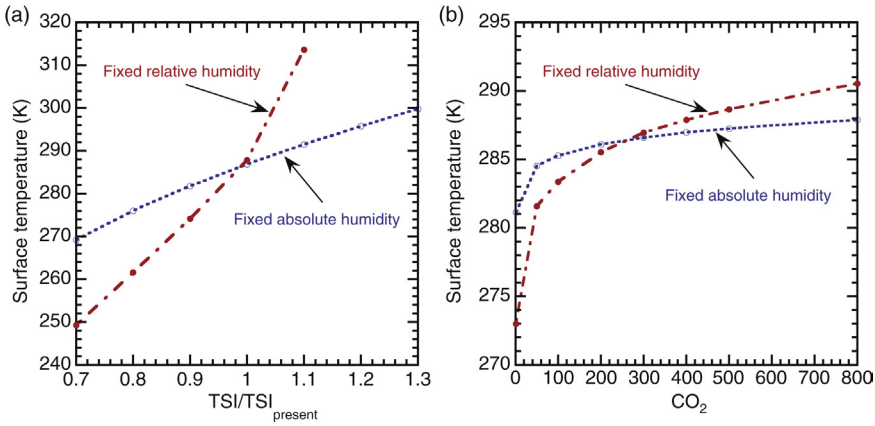


**FIGURE 10.2** **Radiative-convective equilibrium calculation of surface temperature as a function of (a) the ratio of total solar irradiance (TSI) to today's value and (b) as a function of $CO_2$ in ppm.** In each plot one curve shows the result if specific humidity is fixed at today's value and one curve shows the result if relative humidity is fixed at today's value.

the temperature response is not linear because climate forcing from $CO_2$ varies approximately logarithmically with gas concentration, so that increasing the $CO_2$ from 150 ppm to 300 ppm produces the same climate forcing as increasing the $CO_2$ from 300 ppm to 600 ppm.

Figure 10.3 shows OLR as a function of surface temperature obtained from radiative-convective equilibrium calculations such as those shown in Fig. 10.2 in which the model is forced with changing TSI, the relative humidity is assumed fixed and the lapse rate follows the moist adiabat. Except for some unexplained wiggles, the data are fit very well with a line that has a slope of 1.93 W $m^{-2}$ $K^{-1}$. In the background as dotted lines are shown Planck curves for different emission temperatures, $T_e = T_s - \Delta T$, where $\Delta T$ varies from $-15$ to 75 at intervals of 15 K. The slopes of the black body emission curves are much steeper than the radiative convective equilibria, because of strong water-vapor feedback. The OLR from the model varies approximately linearly over a wide range of surface temperature. From radiative-convective equilibrium calculations with FRH we thus obtain an estimate of the climate sensitivity parameter with only the Planck and relative humidity feedbacks included.

$$(\lambda_R)_{FRH} = \left( \left( f \frac{dF^{\uparrow}(\infty)}{dT_s} \right)_{FRH} \right)^{-1} \approx 0.5\,\mathrm{K(W\,m^{-2})^{-1}} \qquad (10.10)$$

Comparing (10.10) with (10.7) we see that adding relative humidity feedback nearly doubles the estimated sensitivity of the climate, which is also consistent with the differences between fixed specific humidity and FRH in Fig. 10.2. With these two feedbacks included, the response of surface temperature to a doubling of $CO_2$ concentration is about 2°C.

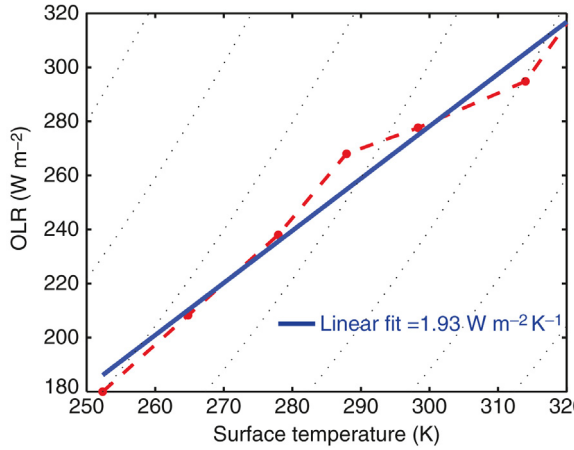


**FIGURE 10.3 A plot of OLR versus surface temperature from a set of one-dimensional radiative–convective equilibrium calculations in which relative humidity is fixed and the moist-adiabatic lapse rate is assumed.** The blue line is the linear fit to the data indicated by the red dots. The dotted lines in the background indicate black body emission curves. The surface temperature was changed by altering the TSI from 70% to 110% of today's value.

An assumption that the relative humidity remains approximately constant when the climate warms or cools has generally been shown to be an excellent approximation. Figure 10.4 shows zonal cross-sections of the relative humidity for the annual mean, January and July. The relative humidity has strong variations with altitude and latitude. Near the surface, the relative humidity is fairly high, except in latitudes with a lot of dry land areas such as the subtropics, especially in the Northern Hemisphere where the subtropical belt (10–40°N) has a large amount of dry land areas over Africa and Asia. In the mid-troposphere, the relative humidity is also very low in the subtropics, where sinking motion takes cold dry air from upper levels and heats it up adiabatically. The stratosphere is very dry, with very low relative humidity, except over the Antarctic in winter. Although the relative humidity has very strong spatial patterns and seasonal variations, these are related to the circulation, which changes only modestly with climate, in comparison to the saturation vapor pressure, which changes rapidly with temperature.

Figure 10.5 shows the spatial distribution of relative humidity at 500 hPa. Again, large regions of the tropics where the average vertical motion is downward have very low relative humidity. It is in these regions with less water vapor and cloud where the Earth can emit radiation to space effectively (compare the relative humidity in Fig. 10.5 with OLR in Fig. 2.10).

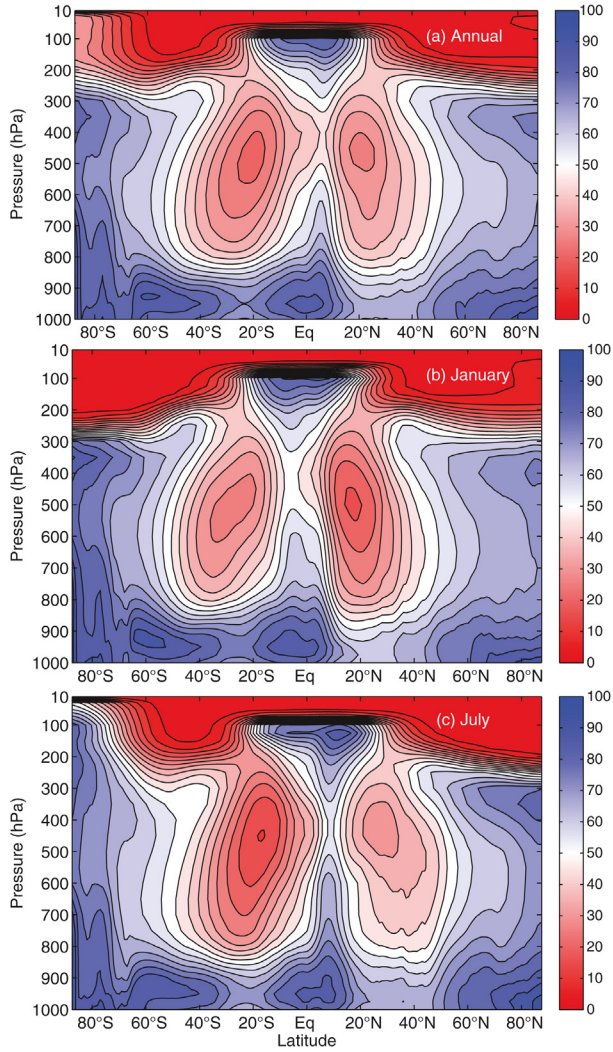


**FIGURE 10.4 Latitude–pressure cross-sections of zonal mean relative humidity for (a) annual mean, (b) January, and (c) July.** Contour interval is 10%. *From ERA Interim reanalysis.*

Emission from these dry zones allows Earth to stay cooler than it would if the water vapor was evenly spread over the surface area of Earth.

### 10.3.3 Lapse-Rate Feedback

Back in Chapters 2 and 3 we showed that the decrease of air temperature with altitude is critical to the greenhouse effect, since greenhouse

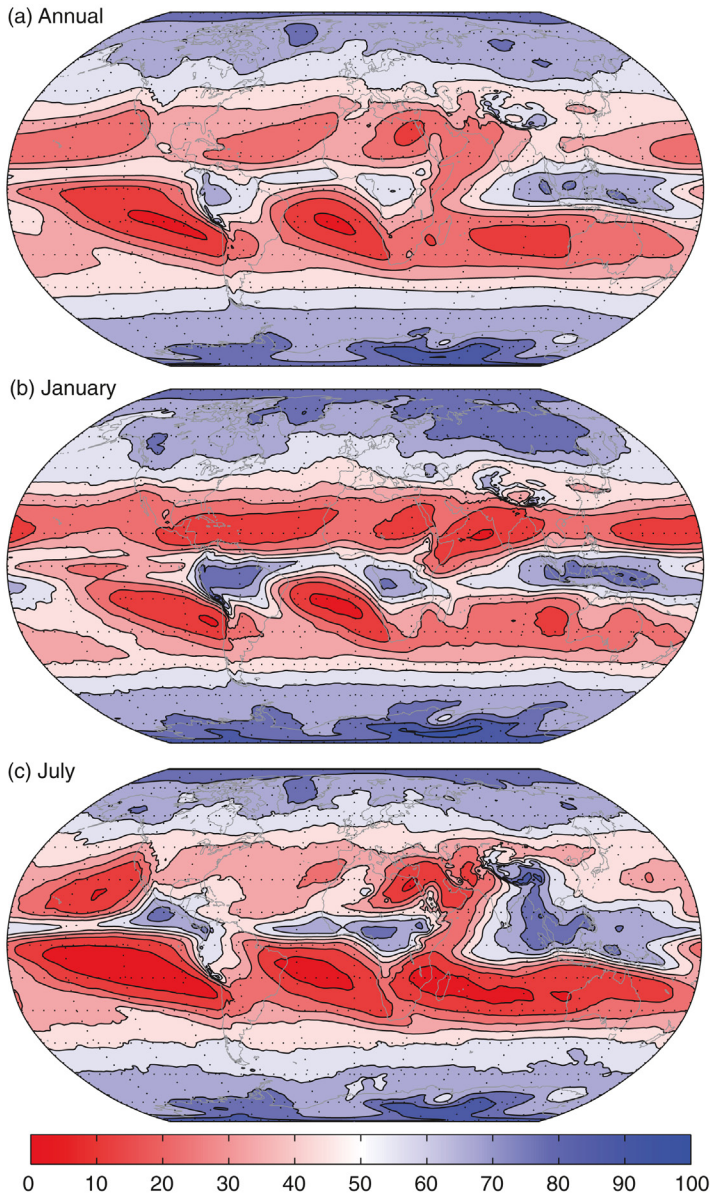


**FIGURE 10.5 Maps of relative humidity at 500 hPa for (a) annual mean, (b) January, and (c) July.** Contour interval is 10%. *From ERA Interim reanalysis.*

gases and clouds cause the emission of thermal infrared radiation by Earth to originate in the middle troposphere, which is cooler than the surface. Therefore, if we weaken the lapse rate, the surface and the emission temperatures become closer together, the greenhouse effect is weakened, and we should expect the surface temperature to cool. So if the lapse rate decreases with increasing surface temperature, that would be a negative feedback, all else being equal. However, all else is not equal.

Because the saturation vapor pressure is strictly a function of temperature only, if the relative humidity is approximately constant, then the water vapor mixing ratio is a function of only temperature. In that case, when you decrease the lapse rate, the air above the surface warms. If the relative humidity is fixed, these warmed layers will also contain more water vapor. If the emission comes from the water vapor and the water vapor is a function of temperature only, then the water vapor that does the emitting stays at about the same temperature, regardless of the lapse rate. If the lapse rate increases, the water vapor decreases where it cools so that the emission comes from lower in the atmosphere, where the temperature is nonetheless about the same as before the lapse rate change. The effect of decreased pressure broadening on the absorption lines of water vapor has a very modest effect as the emission moves to lower pressures. Figure 10.6 illustrates the effect of lapse rate with a simple schematic. As the lapse rate decreases

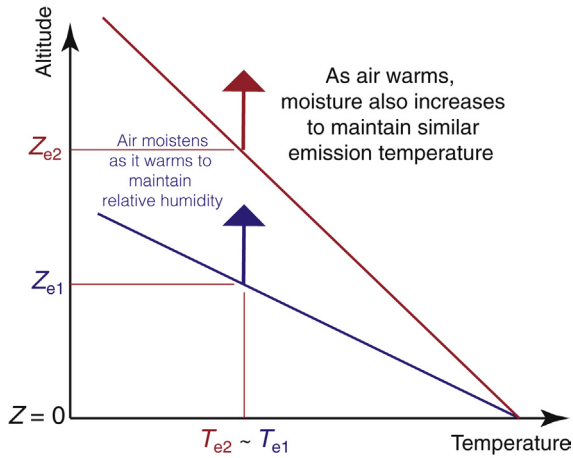


**FIGURE 10.6 Schematic diagram showing how relative humidity feedback offsets the effect of lapse-rate feedback.** Two temperature plots are shown as a function of altitude with larger (blue line) and smaller (red line) lapse rates and the same surface temperature. The emission temperature is marked by the upward-directed arrows. As the lapse rate decreases and the air above the surface warms, the air will also acquire additional water vapor to keep its relative humidity constant. Thus the emission level moves up in altitude and stays at about the same temperature, so that the emission to space is almost independent of the lapse rate, if the relative humidity is fixed.

(red line), the warmed air above the surface gains moisture if the relative humidity is fixed. Then the emission level moves upward and the emission temperature remains nearly constant. Thus the relative humidity feedback cancels the effect of the lapse rate change and the emission to space comes from the same temperature as before the lapse rate changed. For this reason, so long as the relative humidity remains about constant, the effect of lapse-rate feedback will always be greatly muted by the associated water vapor feedback. This was first pointed out by Cess (1975).

## 10.4 ICE–ALBEDO FEEDBACK

The physical effects of expanded surface ice cover have often been offered as one possible explanation for how the very different conditions of the ice ages could have been maintained. One of the primary physical effects of ice cover is the much higher albedo of ice and snow than all other surface coverings (Table 4.2). The annual variation of surface albedo is controlled largely by snow cover (Fig. 4.4). In the Northern Hemisphere, the seasonal variation of surface albedo is large over a wide range of latitudes from 45°N to the pole, whereas in the Southern Hemisphere it is confined to the latitude where seasonal sea ice is present around Antarctic, from 55°S to 75°S (Fig. 10.7). Vegetation cover can also influence the

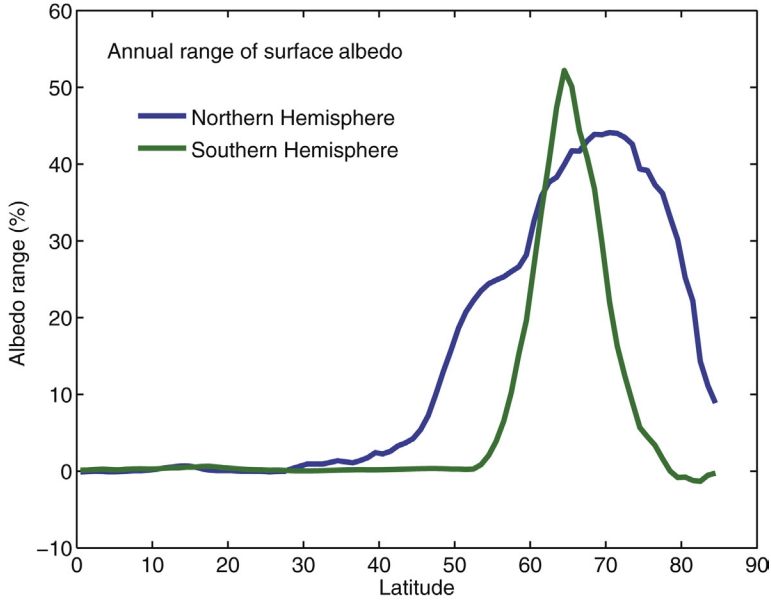


**FIGURE 10.7** **Surface albedo contrast between winter and summer estimated using January and July.** *From NASA-CERES surface radiation budget estimates.*

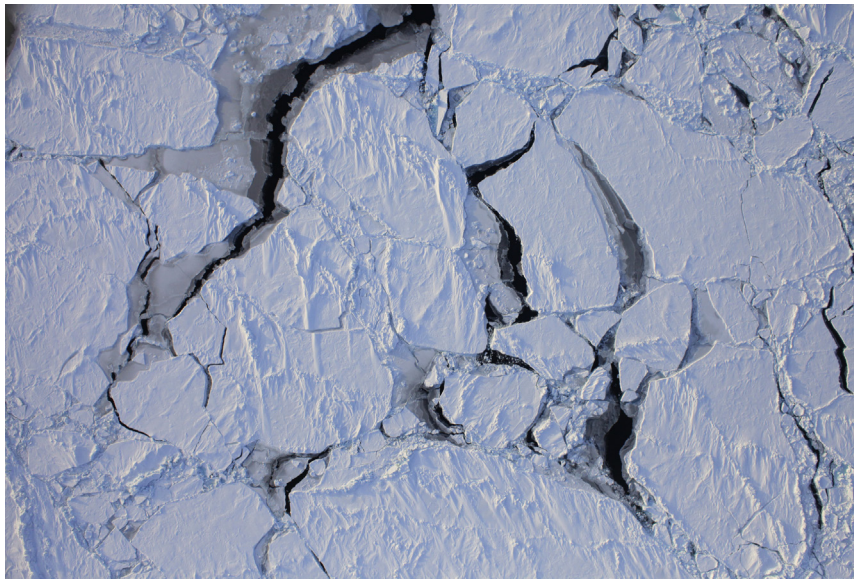

FIGURE 10.8 **Aerial photo of Arctic Sea Ice.** Dark areas are leads where open water is exposed. Features on the ice floes include pressure ridges and snow drifts. *NASA image; courtesy: the Digital Mapping system team and Operation IceBridge Arctic 2011.*

seasonal variation of albedo, and solar zenith angle is also an important influence on seasonal variations of surface albedo in high latitudes. The albedo of ocean surfaces at high latitudes is typically 10%, whereas a typical albedo for sea ice with a covering of snow at the same latitudes is 60% (Fig. 10.8). The surface albedo contrast between coniferous forest and an ice sheet is also very large. Surface albedo variations are muted by the presence of clouds, since when clouds are present the albedo at the top of the atmosphere is already fairly high and changing the surface albedo has a smaller, but still very significant effect, especially since clouds are not always present.

As the climate cools during the onset of an ice age, the ice would expand into regions previously covered by water or forest in latitudes where the insolation is substantial, particularly in summer. The increased surface ice cover would raise the surface albedo and reduce the amount of solar energy absorbed by the planet. This reduction of solar energy absorption would cause further cooling and thus further ice expansion that might ultimately lead to an ice age. The association of surface glaciation with colder temperatures can constitute a very powerful positive feedback, since it modulates the direct energy input from the Sun.

The albedo feedback effect was incorporated in simple climate models by Budyko (1969) and Sellers (1969). Both of their models produce very sensitive climates, such that it is surprisingly easy to produce an ice age, or

even an ice covered Earth, with a relatively modest climate forcing. Their simple models for the ice caps assume that everything about the climate can be characterized by the surface temperature, and that the only independent variable is latitude. The determination of the surface temperature is based on the conservation of energy for the system, so that these models are termed *energy-balance climate models*. The steady-state energy balance has three terms: the absorbed solar energy, the emitted terrestrial energy, and the divergence of the horizontal energy transport by the atmosphere and oceans. Since the growth of polar ice caps and their effect on global climate is the central question that these models are designed to address, and this depends heavily on the sphericity of Earth, these models are functions of latitude on a sphere.

It is convenient to express the three terms in the energy balance as functions of the sine of latitude, $x = \sin \phi$, and the surface temperature $T_s$.

$$Q_{ABS}(x, T_s) - F_{\infty}^{\uparrow}(x, T_s) = \Delta F_{ao}(x, T_s) \tag{10.11}$$

$Q_{ABS}$ is the absorbed solar radiation, $F_{\infty}^{\uparrow}$ is the OLR, and $\Delta F_{ao}$ is the removal of energy by horizontal energy transport, which would usually be expressed as the divergence of the meridional energy transport by the atmosphere and ocean. The observed climatological zonal average values of these terms are shown in Fig. 2.12. The absorbed solar radiation is written as the product of the TSI, $S_0$, a function that describes the distribution of insolation with latitude, $s(x)$, and the absorptivity for solar radiation, $a_p(x, T_s) = 1 - \alpha_p(x, T_s)$, which is one minus the planetary albedo, $\alpha_p$.

$$Q_{ABS}(x, T_s) = \frac{S_0}{4} s(x) a_p(x, T_s) \tag{10.12}$$

The distribution of annual mean insolation is shown in Fig. 2.7. The distribution function $s(x)$ is defined by dividing the annual mean insolation at each latitude by the global average insolation. Its global area average is unity.

$$\frac{1}{2}\int_{-1}^{1} s(x)\, dx = 1 \tag{10.13}$$

The annual mean insolation distribution function for current conditions can be approximated fairly accurately as

$$s(x) = 1.0 - 0.477 P_2(x) \tag{10.14}$$

where

$$P_2(x) = \frac{1}{2}(3x^2 - 1) \tag{10.15}$$

is the Legendre polynomial of second order in $x$.

The emitted terrestrial flux is specified as a linear function of surface temperature.

$$F_{\infty}^{\uparrow}(x, T_s) = A + BT_s \tag{10.16}$$

The coefficients $A$ and $B$ can be obtained from a radiative transfer model, or from observational estimates. The transport then can be specified in two different ways that facilitate an easy solution. Budyko assumed a linear form for the transport term, such that at every latitude, the transport relaxes the temperature back toward its global-mean value,

$$\Delta F_{ao}\big|_{\text{Budyko}} = \gamma(T_s - \tilde{T}_s) \tag{10.17}$$

where

$$\tilde{T}_s = \frac{1}{2}\int_{-1}^{1} T_s \, dx \tag{10.18}$$

is the global mean temperature.

Sellers (1969) and North (1975) used a diffusive approximation to meridional transport.

$$\Delta F_{ao}\big|_{\text{Sellers}} = \nabla \cdot K_H \nabla T_s = \frac{\partial}{\partial x}(1 - x^2) K_H \frac{\partial T_s}{\partial x} \tag{10.19}$$

The linear relaxation coefficient, $\gamma$, and diffusivity, $K_H$, are chosen to make the model simulation as close to the observed climate as possible by producing the observed meridional energy transport when the temperature gradient is approximately as observed.

Albedo feedback is introduced by assuming that ice forms when the temperature falls below a critical value and that this causes an albedo increase. It is observed that the annual mean temperature at which surface ice cover persists throughout the year is about –10°C currently. Therefore, we assume that an abrupt transition in the albedo takes place at this temperature.

$$\alpha_p = \begin{cases} \alpha_{\text{Ice free,}} & T_s > -10^{\circ}\text{C} \\ \alpha_{\text{Ice,}} & T_s < -10^{\circ}\text{C} \end{cases} \tag{10.20}$$

Typical values chosen for planetary albedos with and without surface ice cover are 0.62 and 0.3, respectively.

If we substitute (10.12), (10.16), and (10.17) into (10.11), we obtain the equation considered by Budyko.

$$A + BT_s + \gamma(T_s - \tilde{T}_s) = \frac{S_0}{4} s(x) a_p(x, x_i) \tag{10.21}$$

Here we have used the fact that because of (10.20), the absorptivity is only a function of sine of latitude $x$ and the position of the ice line, $x_i$, the point where the temperature equals –10°C. We define a new variable $I$, which is the ratio of the terrestrial emission to the global average insolation.

$$I = \frac{(A + BT_s)}{(1/4)S_0} \tag{10.22}$$

Substituting this definition into (10.21) yields a simple equation for $I$.

$$I + \delta(I - \tilde{I}) = s(x)a_p(x, x_i) \tag{10.23}$$

It is interesting that the linear parameters describing the efficiency of meridional energy transport and longwave radiative cooling occur only in the ratio $\delta = (\gamma/B)$. If $\delta$ is large, then meridional transport is relatively efficient compared to longwave cooling, and equator-to-pole gradients in $I$ will be small.

The global area average of (10.23) is

$$\tilde{I} = \frac{1}{2}\int_{-1}^{1} s(x)a_p(x, x_i)\,dx. \tag{10.24}$$

which indicates that the global average value of the terrestrial emission divided by the insolation is equal to the global average of the product of the absorptivity and the distribution function for insolation. Thus, if the absorptivity is high where the insolation is also high, the global mean value $I$ will also be high. Since $I$ is linearly related to $T_s$, the global mean temperature also increases with the average product of insolation and absorptivity. Because the annual mean insolation is least at the poles and greatest at the equator, the albedo increase associated with ice cover will have a greater effect on global mean temperature as the ice cover extends farther toward the equator.

It is interesting to solve for the latitude of the ice boundary as a function of TSI for particular albedo specifications and values of $\delta$. The solution is obtained by specifying the position of the ice line and then solving for $I$ at the ice line latitude using (10.23). Because the albedo specification is discontinuous at the ice line and no diffusion is present in the model, $I$ and $T_s$ are discontinuous and the solution for $x_i$ as a function of $S_0$ is not unique. A unique solution can be obtained by adding a small diffusive transport and then taking the limit of vanishing diffusion coefficient. This procedure suggests using the average of the albedo on both sides of the ice edge when solving for $I$ at the ice edge (Held and Suarez, 1974). The general structure of such solutions is shown in Fig. 10.9a. Because of the strong nonlinearity introduced by the albedo specification, the model may have between one

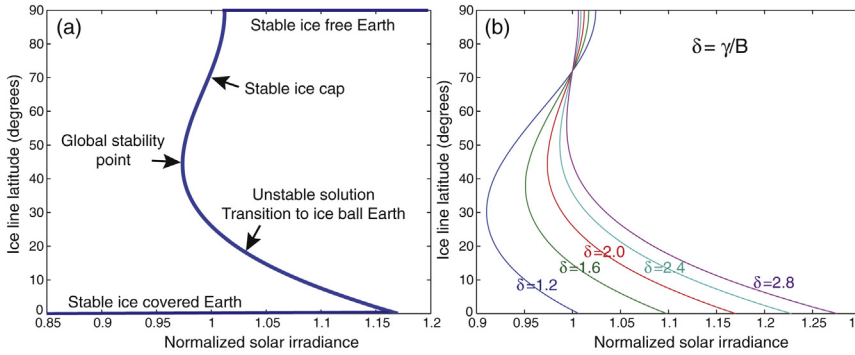


**FIGURE 10.9 Iceline latitude in the Budyko energy balance climate model as a function of normalized TSI.** (a) Schematic diagram showing the stable and unstable solutions for $\delta = 2$, (b) diagram showing the dependence of the ice-line latitude on the ratio of transport to cooling efficiency $\delta = \gamma/B$.

and three solutions for a particular value of the TSI. For sufficiently large TSIs, an ice-free planet is a stable solution to the model. For sufficiently small TSIs, an ice-covered planet is a stable solution. For an intermediate range of TSIs both of these stable solutions are possible.

The diagram has been scaled such that for a normalized TSI of 1.0 the boundary of the polar ice cap is at 72°N, which is approximately the current position of the ice edge. If the TSI is raised or lowered from this value the ice cap will recede or expand. The rate at which the ice cap expands or contracts as the TSI is changed is a measure of the sensitivity of the climate. This rate is equivalent to the slope of the solution curve for the stable ice cap in Fig. 10.9. As the TSI is decreased and the ice cap expands, the model becomes more sensitive until the line is vertical at some critical latitude. The latitude where the slope becomes infinite is labeled the global stability point in Fig. 10.9a. From that point, if the solar irradiance is reduced further the ice cap moves to the equator, yielding the snowball Earth condition. The intervening steady state solution indicated in the diagram shows the ice edge moving equatorward with increasing solar irradiance, which is unphysical, and these solutions are unstable. The point where this solution branch reaches the equator, though, marks the amount by which the solar irradiance must be increased to make an ice-covered planet transition to an ice-free solution. The model thus indicates hysteresis, whereby once the planet is ice-covered by reducing the solar irradiance to 98%, it must then be increased to 117% to get the ice to melt, at which point it melts completely. To get an ice cap to form again, the solar irradiance must be reduced to about 102% (Fig. 10.9a).

The parameters chosen by Budyko (1969) and Sellers (1969) make the ice cap very sensitive to small changes in TSI. For example, Budyko

calculated that a reduction in TSI of 1.6% would lead to an ice covered Earth. This result is attractive in that it indicates that a relatively small change in climate forcing could produce the glacial–interglacial transitions that have occurred during Earth history. On the other hand, the global stability point is reached when the ice cap has expanded to about 45° latitude. The inference from this simple model is thus that during glacial maxima, when the average latitude of perennial ice cover was near midlatitudes, the planet is very close to making an irreversible transition to an ice-covered condition. Energy balance climate models are extremely simple, of course, and neglect many important processes, but it is still interesting to see how their sensitivity depends on the parameters needed for their solution.

We may first examine how the sensitivity of the model depends on the parameter $\delta$, which measures the ratio of the meridional transport coefficient, $\gamma$, to the longwave radiative cooling coefficient, $B$. Figure 10.9b shows a set of solution curves for selected values of $\delta$. For larger values of $\delta$ the boundary of a small polar ice cap is more sensitive to TSI changes. This is related to the fact that large values of $\delta$ produce weak meridional temperature gradients; so that a small change in global mean temperature is translated into a large displacement of the ice line and thereby a large change in absorbed solar radiation. Budyko used a value of $B = 1.45$ W m$^{-2}$ K$^{-1}$, whereas more recent estimates would place the most appropriate value closer to 2.2 W m$^{-2}$ K$^{-1}$. The resulting value of $\delta$ in Budyko's calculation was 2.6. This high value of $\delta$ contributed to the great sensitivity of his model.

The planetary albedo contrast associated with surface ice cover is also a critical parameter controlling the sensitivity of energy balance climate models. The increase of planetary albedo with latitude is an observed fact (Fig. 2.9), but only a portion of this meridional increase of planetary albedo is associated with surface ice. Significant contributions are also made by the increase of cloud cover with latitude (Fig. 3.21) and the increase of the albedo with solar zenith angle, which also increases with latitude (Fig. 2.8). As a result the ice-free albedo increases with latitude, so that in the latitudes where ice is likely to form, the contrast of planetary albedo between ice-free and ice-covered conditions is not as great as one might expect on the basis of the surface albedo change. Much of the surface albedo increase is screened by clouds, which are very good reflectors of solar radiation, particularly at high solar zenith angles. One may take this into account in the energy balance climate model by assuming that the ice-free absorptivity for solar radiation decreases with latitude. A realistic appraisal of ice–albedo feedback is that, although it is an important feedback process, it is not strong enough by itself to explain the ease with which the climate system appears to change from glacial to interglacial conditions.

## 10.5 DYNAMICAL FEEDBACKS AND MERIDIONAL ENERGY TRANSPORT

In the energy-balance climate models, the efficiency of meridional energy transport and the resulting meridional temperature gradient play an important role in determining the sensitivity of climate. It is interesting to consider how meridional energy transport in the atmosphere and ocean might respond to a developing ice sheet or to some other forcing of the meridional temperature gradient. If we limit ourselves to midlatitudes, the biggest contribution to meridional energy transport comes from eddies in the atmosphere (Chapter 6). The dependence of the eddy fluxes of heat on the mean temperature gradients can be estimated from simple dimensional arguments. We first suppose, as was done by Sellers (1969) and North (1975), that the meridional energy transport depends on the meridional gradient of potential temperature, $\Theta$.

$$[v'\Theta'] = -K_H \frac{\partial \Theta}{\partial y} \tag{10.25}$$

where square brackets indicate a zonal average and $y$ is the northward displacement in a local Cartesian coordinate system. The transport coefficient $K_H$ must have the units of $m^2\ s^{-1}$, so we can think of $K_H$ as the product of a characteristic wind speed $V$ and distance $L_e$.

$$K_H \propto V \times L_e \tag{10.26}$$

The eddy heat fluxes are produced by disturbances that result from baroclinic instability of the zonal average state of the atmosphere, so we use the theory for baroclinic instability to select the characteristic wind speed and length scales. The length scale is chosen to be the Rossby radius of deformation, which is approximately the scale of disturbances that grow most rapidly in response to the baroclinic instability of the zonal mean flow (Holton and Hakim, 2012).

$$L_e \approx L_R = \frac{N d_e}{f} \tag{10.27}$$

where $d_e$ is the depth scale for the disturbance, $f$ is the Coriolis parameter, and $N$ is the buoyancy frequency, which is related to the vertical gradient of the potential temperature.

$$N^2 = \frac{g}{\Theta} \frac{\partial \Theta}{\partial z} \tag{10.28}$$

The appropriate wind speed scale is the difference in zonal mean wind speed experienced by the eddy across its vertical extent, $d_e$.

$$V = d_e \left| \frac{\partial u}{\partial z} \right| \tag{10.29}$$

The vertical shear of the zonal mean wind is related to the meridional gradient of potential temperature by the thermal wind approximation, which is accurate away from the equator.

$$\frac{\partial [u]}{\partial z} \approx -\frac{g}{f[\Theta]} \frac{\partial [\Theta]}{\partial y} \tag{10.30}$$

Combining (10.25) through (10.30), we obtain an expression for the meridional flux of dry static energy by transient eddies as a function of the mean state variables.

$$[v'\Theta'] \approx -\left( \frac{g}{[\Theta]} \right)^{3/2} \frac{d_e^2}{f^2} \left( \frac{\partial [\Theta]}{\partial z} \right)^{-1/2} \left| \frac{\partial [\Theta]}{\partial y} \right| \frac{\partial [\Theta]}{\partial y} \tag{10.31}$$

The conservation of potential temperature can be used to scale the characteristic vertical velocity and characteristic vertical-length scale to the horizontal velocity and length scales.

$$W = V \left| \frac{\partial [\Theta]}{\partial y} \right| \left| \frac{\partial [\Theta]}{\partial z} \right|^{-1} \tag{10.32}$$

Using this scaling of the vertical velocity, we can obtain an expression for the vertical heat flux analogous to (10.31).

$$[w'\Theta'] \approx -\left( \frac{g}{[\Theta]} \right)^{3/2} \frac{d_e^2}{f^2} \left| \frac{\partial [\Theta]}{\partial y} \right|^3 \left( \frac{\partial [\Theta]}{\partial z} \right)^{-1/2} \tag{10.33}$$

According to these scaling arguments, the magnitude of the meridional eddy heat flux is proportional to the square of the meridional temperature gradient and to the square root of the static stability (10.31). The depth scale $d_e$ is as yet unspecified. Strongly unstable disturbances occupy the entire troposphere, so that it is reasonable to use the scale height $H$ as the depth scale. For more weakly unstable flows the depth scale itself is proportional to the meridional temperature gradient, so that the total heat flux is even more highly sensitive to the meridional temperature gradient (Held, 1978). Because of the quadratic or higher dependence of the eddy heat flux on the meridional temperature gradient, eddy fluxes act to suppress large deviations of the meridional temperature gradient, so that, to the extent that the meridional temperature gradient is controlled by eddy fluxes, we expect the meridional gradient of atmospheric temperature to be rather insensitive to altered thermal driving of the equator-to-pole

temperature difference. Altered meridional thermal drive will result in a large change in baroclinic eddy activity and eddy heat transport, which will suppress the response of the temperature gradient to the altered forcing. The strong sensitivity of the eddy activity and heat flux to meridional thermal driving has been verified by calculations with numerical models of the atmosphere.

We expect that the oceanic heat flux is also sensitive to the meridional temperature gradient, since we expect that both the thermal driving and the wind stress driving of oceanic circulations would increase with the temperature gradient. We do not have any simple quantitative theory for how oceanic fluxes depend on the meridional temperature gradients that corresponds to the simple dimensional arguments given above.

Dynamical models of the free atmosphere suggest that baroclinic eddies will act to maintain a nearly constant meridional temperature gradient by changing their meridional energy flux by a large amount when a small change in meridional temperature gradient is imposed. It is very interesting that paleoclimatic data show that the surface temperature has a very different behavior than expected from these dynamical considerations. During ice ages, the tropical surface temperatures changed only a few degrees from today's values, whereas the polar temperatures cooled by 10°C or more. This "polar amplification" of climate change is an important feature that needs to be fully understood. It points to the importance of surface and boundary layer processes in determining the surface temperature and its latitudinal gradient, or to a strong latitude dependence of feedback processes. Much of the enhanced temperature change in high latitudes appears to be confined near the surface, so that polar amplification of surface temperature change and the hyperdiffusive theory for heat flux described previously are not inconsistent. The meridional gradients of mean tropospheric temperature change much less than the meridional gradients of surface temperature in climate models, so that much of the polar amplification of warming is confined to the lower troposphere.

## 10.6 LONGWAVE AND EVAPORATION FEEDBACKS IN THE SURFACE ENERGY BALANCE

The energy and water exchanges at the surface are very important for climate (Chapter 4), and it is of great interest to understand how these energy exchanges might be sensitive to temperature. We can gain some intuition about this through relatively simple analysis.

The net longwave heating of the surface is equal to the downward longwave from the atmosphere minus the longwave emission from the surface.

$$F^{\downarrow}_{\text{Net}} = F^{\downarrow}(0) - \sigma T_s^4 \tag{10.34}$$

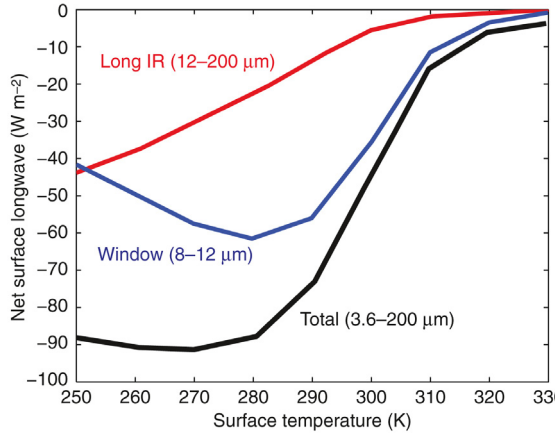


**FIGURE 10.10 Net longwave at the surface as a function of surface temperature calculated from a radiative transfer model.** Separate curves are shown for the total longwave, the window region (8–12 μm) and the longest IR wavelengths that are of importance where the rotational lines of water vapor produce strong absorption and emission (12–200 μm).

Here we have assumed that the surface absorbs and emits like a blackbody. We can calculate the dependence of net radiation on surface temperature under clear-sky conditions using a radiative transfer model with some assumptions. We assume that the temperature decreases linearly with height away from the surface with a lapse rate of 6.5 K $km^{-1}$ until the height where the temperature reaches a minimum of 200 K, and that the atmosphere is isothermal with a temperature of 200 K above that level. We assume that the relative humidity is distributed linearly in pressure according to

$$\mathrm{RH} = \mathrm{RH}_o \left( \frac{p/p_s - 0.02}{1 - 0.02} \right) \tag{10.35}$$

where $\mathrm{RH}_o = 77\%$ gives a reasonable approximation to the observed global mean relative humidity. The net longwave flux at the ground computed with these specifications of lapse rate and relative humidity and with current values of $CO_2$ and ozone content is shown in Fig. 10.10. The general character of this plot is not very sensitive to the details of how the relative humidity and temperature profiles are specified. For temperatures less than about 280 K the net longwave loss from the surface is about 90 W $m^{-2}$ and is not sensitive to temperature. This is because there is very little water vapor in the atmosphere at these temperatures and the downward longwave from the atmosphere and the upward longwave from the surface

increase at about the same rate, so that the balance remains the same. For temperature greater than about 280 K, as the temperature increases the net longwave loss from the surface decreases. In this temperature range, the infrared opacity of the water vapor begins to increase rapidly, if the relative humidity is fixed. This means that the downward longwave emission from the atmosphere increases more rapidly with temperature that the upward blackbody emission from the surface. At tropical temperatures of about 300 K, the surface longwave loss is decreasing rapidly, changing from about $-75$ W m$^{-2}$ at 290 K to about $-15$ W m$^{-2}$ at 310 K, or about $+3$ W m$^{-2}$ K$^{-1}$. From the atmosphere's perspective, this change in the surface longwave exchange is a loss of energy, since the amount of longwave energy that it emits downward is increasing faster than the amount it receives from the surface. Much of the reduction in net longwave cooling of the surface comes from wavelengths in the range 8–12 μm, called the water vapor window. This is because of the so-called continuum absorption by water vapor that becomes increasingly effective at high vapor pressure. The nature of this absorption is not fully understood, but it is well measured and likely associated with water vapor molecules sticking together at high vapor pressures, and thus forming a complex molecule that can efficiently absorb and emit window radiation. This closes the water-vapor window at high temperatures and makes the cloud-free atmosphere virtually opaque to thermal infrared radiation. According to these calculations, upward and downward longwave radiation at the surface would become almost equal for surface temperatures in excess of ~320 K. The net surface longwave loss decreases most rapidly with temperature in the vicinity of 300 K, which is approximately the mean temperature of the tropical oceans. This constitutes a positive feedback in the surface energy budget that is most effective at tropical temperatures, since as the temperature increases the net longwave cooling of the surface decreases. If no other feedback processes were operating, the tropical sea surface temperature (SST) might be quite sensitive and variable.

The approximate energy balance of the tropical ocean surface is about 200 W m$^{-2}$ solar heating, balanced by 120 W m$^{-2}$ evaporative cooling, 50 W m$^{-2}$ net longwave loss, 10 W m$^{-2}$ sensible cooling, and 20 W m$^{-2}$ energy export by ocean currents. The evaporative cooling of tropical ocean waters is the largest cooling term. It is much greater than the longwave cooling and is sensitive to surface temperature. We can estimate the sensitivity of evaporative cooling to surface temperature if we are willing to make several critical assumptions. We begin with the aerodynamic formula for evaporative cooling approximated using (4.32) and (4.35).

$$\mathrm{LE} = \rho_a L C_{DE} U q_s^* \left( (1 - \mathrm{RH}) + \mathrm{RH} \left( \frac{L}{R_v T_s^2} \right) (T_s - T_a) \right) \tag{10.36}$$

If we assume again that the RH distribution and the temperature profile remain constant as we increase the surface temperature, then the evaporative cooling depends primarily on the temperature dependence of the saturation specific humidity at the surface. We can also assume that the characteristic wind speed and the exchange coefficient are independent of the surface temperature. Making these assumptions and neglecting the weaker linear and quadratic temperature dependencies compared to the exponential temperature dependence of saturation humidity, one can show from (10.36) and (4.35) that the logarithmic derivative of evaporative cooling with respect to surface temperature is only weakly dependent on temperature itself.

$$\frac{1}{\mathrm{LE}}\frac{\partial \mathrm{LE}}{\partial T_s} \approx \frac{L}{R_v T_S^2} \approx 6\%\ \mathrm{K}^{-1} \tag{10.37}$$

This is a result of the exponential dependence of saturation humidity. The derivatives of exponential functions are themselves exponential functions. The numerical estimate in (10.37) is obtained for $T_s$ = 300 K, which is a typical tropical oceanic surface temperature. If we multiply (10.37) by a typical evaporative cooling value of LE = 120 W m$^{-2}$, then we obtain an estimate of the sensitivity that is independent of specific choices of the parameters in the aerodynamic formula (10.36).

$$\frac{\partial \mathrm{LE}}{\partial T_s} \approx 7\,\mathrm{W\,m^{-2}\,K^{-1}} \tag{10.38}$$

For FRH, the rate at which evaporative cooling increases with temperature is large compared to the rate at which the longwave cooling of the surface decreases.

Figure 10.10 can be used to calculate the dependence of net longwave cooling on temperature for cloud-free conditions. The maximum rate of change of net longwave heating of the ground occurs at about $T_s$ = 305 K and has a numeric value of

$$\frac{\partial F_{\mathrm{Net}}^{\downarrow}(z=0)}{\partial T_s} \approx 3\,\mathrm{W\,m^{-2}\ K^{-1}} \tag{10.39}$$

The magnitude of the rate of increase of evaporative cooling with temperature is more than double the rate of decrease of the longwave cooling of the surface in our simple analysis here. The ocean surface gradually loses its ability to cool by longwave radiative emission as the temperature increases above 300 K, but the evaporative cooling increases more rapidly with temperature than the longwave cooling declines with temperature. The sensitivity parameter for tropical sea surface

(TSS) conditions obtained by including only these two feedbacks is rather small.

$$(\lambda_R)_{TSS} = \left\{ \frac{\partial LE}{\partial T_s} - f \frac{\partial F_{Net}^{\downarrow}(z=0)}{\partial T_s} \right\}^{-1} \approx 0.3\ K(W\ m^{-2})^{-1} \tag{10.40}$$

If surface longwave heating and evaporation vary with temperature as these simple estimates suggest, tropical SST will be relatively stable. This stability, which is rooted in the rapid change of saturation vapor pressure at tropical surface temperatures, may explain why tropical SST has changed relatively little in the past. It may also contribute to the apparent polar amplification of surface temperature changes by providing a tropical damping of temperature changes.

Evaporative cooling of the tropical ocean surface is very sensitive to the thermodynamic properties of the atmospheric boundary layer, which are determined through a complex interaction among boundary-layer turbulence, mesoscale convection, and large-scale flow. One may illustrate the potential importance of relative humidity variations by differentiating (10.36) with respect to relative humidity for fixed temperature.

$$\left( \frac{\partial LE}{\partial RH} \right)_{T_s} \approx \frac{-LE}{(1-RH)}\% \approx -8\,W\,m^{-2}\,\%^{-1} \tag{10.41}$$

For tropical conditions, the effect on the evaporation rate of a 1 K increase in temperature at FRH is approximately equal and opposite to the effect of a 1% increase in relative humidity at fixed temperature. The processes that control relative humidity in the tropical boundary layer are extremely important to the sensitivity of climate.

The rate of evaporation increase in (10.37) is not likely to be achieved in the global climate system because of the limitations of the atmospheric energy balance. Globally, evaporation must increase only at the rate at which it can be balanced by radiative cooling of the atmosphere (6.3), and the radiative cooling rate of the atmosphere only increases at 1–2% $K^{-1}$ in climate models. In climate models, the relative humidity at the surface over the oceans increases with warming so that the evaporation increase is limited to what the atmosphere can dispose of energetically.

## 10.7 CLOUD FEEDBACK

According to the numbers presented in Table 3.2, clouds double the albedo of Earth from 15% to 30% and reduce the longwave emission by about 30 W $m^{-2}$. Because of the partial cancellation of these two effects,

the effect of clouds on the global net radiative energy flux into the planet is a reduction of about 20 W $m^{-2}$. The effect of an individual cloud on the local energy balance depends sensitively on its height and optical thickness, the insolation, and the characteristics of the underlying surface. For example, a low cloud over the ocean will reduce the net radiation substantially, because it will increase the albedo without much affecting the longwave flux at the top of the atmosphere. On the other hand, a high, thin cloud can greatly change the longwave fluxes without much affecting the solar absorption, and will therefore increase the net radiation and lead to surface warming.

If the amount or type of cloud is sensitive to the state of the climate, then it is possible that clouds provide a very strong feedback to the climate system. Since the fractional area coverage of cloud, $A_c$, is about 50%, and the net effect of this cloud on the energy balance is about –20 W $m^{-2}$, we can make the crude estimate that

$$\frac{\partial R_{\mathrm{TOA}}}{\partial A_{\mathrm{c}}} \approx \frac{\Delta R_{\mathrm{TOA}}}{A_{\mathrm{c}}} \approx \frac{-20\,\mathrm{W\,m^{-2}}}{0.5} = -40\,\mathrm{W\,m^{-2}} \tag{10.42}$$

Thus, a 10% change in cloudiness has the same magnitude of effect on the energy balance as a doubling of $CO_2$ concentration. Increasing the cloudiness by 10 would offset the effect of $CO_2$ doubling. Decreasing the cloudiness by 10% would double the effect of $CO_2$ doubling. If the cloud type changed in such a way as to decrease the shortwave cloud forcing by 5% and increase the longwave cloud forcing by 5%, this would also have the same effect as doubling the $CO_2$ concentration. This could be achieved by decreasing the area coverage and raising the mean cloud top height. Therefore, both the cloud amount and the distribution of cloud types are extremely important for climate. The effect of cloud feedback on the sensitivity of climate is highly uncertain, but we will discuss estimates from current global climate models in Chapter 11.

## 10.8 BIOGEOCHEMICAL FEEDBACKS

The climate of Earth has been shaped by life, and it is certain that biology plays a role in the sensitivity of climate. There are many ways that plants and animals can influence climate sensitivity. Perhaps the strongest and most direct means by which organisms affect climate is through their control of the composition of the atmosphere. The concentration of $CO_2$ in the atmosphere is determined by a complex set of processes, but a key process is the uptake of $CO_2$ by plankton in the surface ocean and plants on land. It is estimated that up to half of the global cooling during the last glacial maximum was contributed by the reduction in atmospheric $CO_2$

concentration This reduction in atmospheric $CO_2$ must have been produced by an alteration in the biology and chemistry of the oceans, since on these time scales atmospheric $CO_2$ is controlled by the partial pressure of $CO_2$ in surface waters.

Sea salt particles and other biological materials contribute cloud condensation nuclei over the oceans. Another important source of condensation nuclei for cloud droplets is the production of sulfurous gases such as dimethyl sulfide by tiny organisms in the surface waters. In the atmosphere, these sulfur-bearing gases are converted into sulfuric acid particles, which form the nuclei around which cloud droplets form by condensation of water vapor. If more of these particles are present, more cloud droplets will form. Because the droplets also tend to be smaller when more condensation nuclei are available, the cloud droplets tend to remain in the atmosphere longer before coagulating and falling out as rain. Also, if the cloud water is spread over more droplets, the albedo of the cloud will be higher (Fig. 3.14). We expect that larger production of sulfur gases that are the precursors of cloud condensation nuclei will lead to higher oceanic cloud albedos and thereby to a cooling of Earth. If the rate at which the organisms release sulfur gases is dependent on temperature, we have the elements of a feedback mechanism. The magnitude of this possible feedback mechanism has not been quantified, and the sign of the feedback is also unknown.

Lovelock (1979) has argued that it may be appropriate to think of Earth as a single complex entity involving the biosphere, atmosphere, ocean, and land, which can be called *Gaia*, the Greek word for "Mother Earth". It is further hypothesized that the totality of these elements constitutes a feedback system, which acts to optimize the conditions for life to exist here. Active control to maintain relatively constant conditions is described by the term *homeostasis*.

Watson and Lovelock (1983) have offered Daisyworld, a simple heuristic model for how life might maintain a very stable climate. They imagine a cloudless planet with an atmosphere that is completely transparent to radiation. The only plants are two species of daisies: one dark (say, black) the other light (say, white) in color. One species reflects less solar radiation than bare ground; the other reflects more. The daisy population is governed by a differential equation for each species.

$$\frac{dA_w}{dt} = A_w(\beta x - \chi) \tag{10.43}$$

$$\frac{dA_b}{dt} = A_b(\beta x - \chi) \tag{10.44}$$

where: $A_w$, $A_b$, and $A_g$ are the fractional areas covered by white daisies, black daisies, and bare ground, respectively; $\beta$ is the growth rate of daisies

per unit of time and area; $\chi$ is the death rate per unit time and area; and $x$ is the fractional area of fertile ground uncolonized by either species.

The growth rate is assumed to be a parabolic function of the local temperature $T_i$, which has a maximum value of one at 22.5°C and goes to zero at 5°C and 40°C.

$$\beta_i = 1.0 - 0.003265(295.5\ \mathrm{K} - T_i)^2 \tag{10.45}$$

The planet is assumed to be in global energy balance, such that

$$\sigma T_e^4 = \frac{S_0}{4}(1 - \alpha_p) \tag{10.46}$$

The planetary albedo $\alpha_p$ is the area-weighted average of the albedos of bare ground, white daisies, and black daisies.

$$\alpha_p = A_g\alpha_g + A_w\alpha_w + A_b\alpha_b \tag{10.47}$$

It is necessary to decide how the local temperatures $T_i$ are to be determined. One extreme is to have all local temperatures equal to the emission temperature $T_e$. This corresponds to perfectly efficient horizontal transport of heat. The other extreme is for each surface type to be at its own radiative equilibrium temperature. This would correspond to no transport of heat between regions with different surface coverings, so that the local temperature is that necessary to balance the local absorption of solar radiation.

$$T_i^4 = \frac{S_0}{4\sigma}(1 - \alpha_i) \tag{10.48}$$

Combining (10.48) with (10.46) yields an expression that satisfies both the local and global energy balance.

$$T_i^4 = \frac{S_0}{4\sigma}(\alpha_p - \alpha_i) + T_e^4 \tag{10.49}$$

We can generalize (10.49) by writing,

$$T_i^4 = \eta(\alpha_p - \alpha_i) + T_e^4 \tag{10.50}$$

where $0 < \eta < (S_0/4\sigma)$ represents the allowable range between the two extremes in which horizontal transport is perfectly efficient, $\eta = 0$, and horizontal transport is zero $\eta = (S_0/4\sigma)$.

Steady-state solutions for Daisyworld can be obtained for specific values of the parameters. Figure 10.11a shows the solution for daisy area and temperature as a function of solar luminosity (TSI) for the case in which the daisies are neutral, because their albedo is the same as the

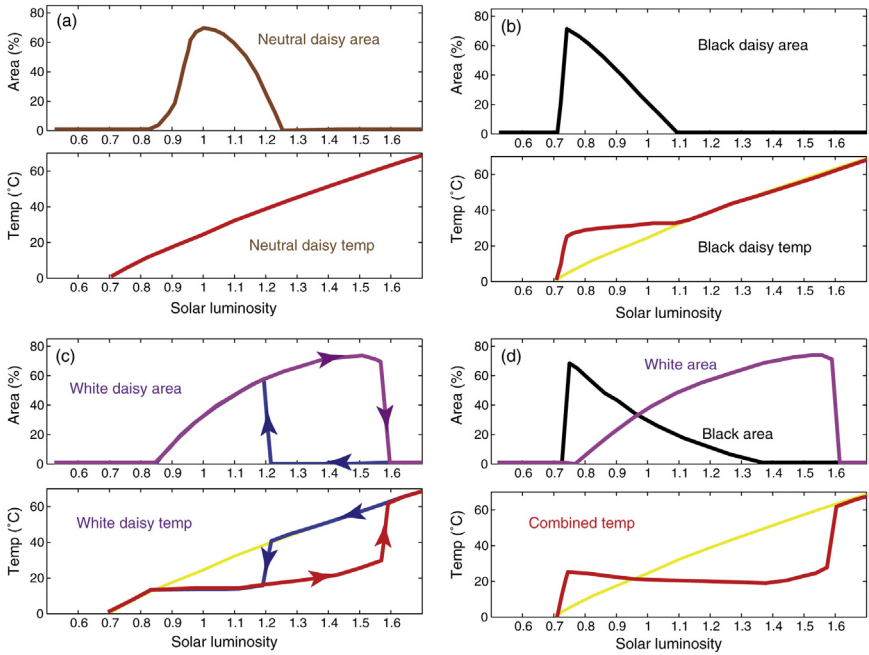


**FIGURE 10.11 Steady-state responses of Daisyworld.** Areas of daisies and global surface temperature are plotted as functions of normalized solar luminosity. The solutions were obtained with a TSI of $S_0 = 1368$ W m$^{-2}$, a bare ground albedo of $\alpha_g = 0.5$, a daisy death rate of $\gamma = 0.3$, and a heat exchange parameter of $\eta = 2.0 \times 10^9$ K$^4$ = 0.12 ($S_0/4\sigma$). (a) For a population of 'neutral' daisies with $\alpha_i = 0.5$; (b) for a population of black daisies with $\alpha_b = 0.25$; (c) for a population of white daisies with $\alpha_w = 0.75$ (note that this shows the evolution for both increasing and decreasing solar constant and that the system exhibits hysteresis); (d) for a population of both black and white daisies. Yellow line repeats the neutral daisy temperature from panel (a). *Adapted from Watson and Lovelock (1983). Reprinted with permission from Munksgaard International Publishers Ltd.*

daisy-free land. In this case, the daisy area increases within the temperature range where daisies can survive, but the daisies do not affect the climate. Figure 10.11b shows what happens if the daisies have an albedo that is 0.25 less than the daisy-free land – black daisies. In this case, as soon as the planet is warm enough for daisies to live, their area increases, which lowers the albedo and warms the planet. If the TSI is raised further, less daisy area results and this keeps the planetary temperature fairly constant until no daisies can exist and the temperature follows the same curve as it does for neutral daisies. For white daisies with an albedo of 0.75, a similar stabilization of temperature occurs as soon as daisies can exist and continues until it is too warm for daisies (TSI ~ 1.55), at which

point the temperature rises abruptly as the daisies disappear (Fig. 10.11c). If the TSI is then lowered, white daisies do not appear until it becomes cool enough for daisies to exist (TSI ~ 1.2) when daisies appear again and the temperature declines. The system thus exhibits hysteresis. White daisies can maintain cool temperatures to a fairly high TSI, because they reflect lots of sunlight, but once they are gone they cannot reappear until the TSI is much lower than when they disappeared. If both black and white daisies are present, the black daisies are favored by low TSI, the white daisies by high TSI and together they keep the climate fairly constant over a wide range of TSI (Fig. 10.11d).

Because of the strong feedbacks within the system, the global mean emission temperature is remarkably stable over a wide range of TSIs within which daisies can exist. These stable regions are bounded by values of TSI where daisies appear or disappear almost discontinuously and temperature takes a corresponding jump. The stable region exists because changes in temperature cause changes in daisy population that produce a strong negative feedback on the temperature. For example, as the insolation increases, white daisies are favored because they are cooler than the emission temperature. The increase in white daisy population increases the planetary albedo, which reduces the response of the emission temperature to the TSI increase.

Daisyworld is certainly not a good representation of Earth, but it serves to illustrate how biology, simply by doing what is natural for it, can influence the global climate and its stability. Biological mechanisms do operate on Earth that could play the role of the daisies on Daisyworld, although it is likely that their effect would be more subtle and muted. For example, the role of biology in controlling $CO_2$ might act like the white daisies, since, once photosynthetic life developed, $CO_2$ was drawn out of the atmosphere. Models suggest that the development of land plants led to a reduction in atmospheric $CO_2$ in the Paleozoic that helped to offset warming associated with increasing TSI (Berner, 1993). In the Daisyworld model, biological processes are hypothesized to be strongly stabilizing, but $CO_2$ changes on glacial–interglacial time scales during the quaternary have done just the opposite by contributing significantly to the sensitivity of climate. Clouds might be the earthly counterpart of the white daisies, with their biological connection coming through the production of cloud condensation nuclei by life in the sea. If the release of dimethyl sulfide (DMS) is proportional to the temperature, then the DMS-cloud albedo connection could constitute a strong negative feedback (Charlson et al., 1987). The sign and magnitude of the climate feedback associated with biological production of cloud condensation nuclei are both uncertain; however, since ocean biology is the primary source of cloud condensation nuclei over the ocean, it seems very likely that the cloud contribution to albedo would be less without life.

## EXERCISES

1. Derive (10.5) from (10.3).
2. Derive (10.9) from (10.8).
3. If equilibrium is defined by $T_s = \sqrt[4]{N+1}\, T_e$ from Section 3.8, then what is the sensitivity parameter $\lambda_R$ in (10.6)? First derive a formula, then compute a numerical value for $N = 3$. Compare with (10.7) and explain the difference.
4. Assume that transient eddies are the primary heat transport mechanism determining vertical and horizontal potential temperature gradients in midlatitudes, and that the eddy transports respond to the mean gradients as indicated by (10.31) and (10.33). If the radiative forcing of the meridional gradient produces a larger equator-to-pole heating contrast, how will the vertical gradient of potential temperature (static stability) in midlatitudes respond? Will the change in static stability be relatively large or small compared to the change in meridional temperature gradient? Assume that potential temperature is relaxed linearly toward a radiative equilibrium value and that the relaxation rate of vertical and horizontal gradients is the same.
5. Use the Budyko energy-balance climate model (10.23) to solve for the TSI as a function of iceline latitude. Use (10.14) and the parameters $B = 1.45$ W m$^{-2}$ K$^{-1}$, $a_0 = 0.68$, $b_0 = 0.38$, and $a_2 = 0.0$. Plot the curves for two values of $\gamma$; $\gamma = 3.8$ W m$^{-2}$ K$^{-1}$ and $\gamma = 2.8$ W m$^{-2}$ K$^{-1}$.
6. According to the energy-balance climate models with ice–albedo feedback, how does the sensitivity of climate relate to the meridional temperature gradient in equilibrium? As the meridional temperature gradient increases, does the climate become more or less sensitive, assuming an ice cap is present?
7. Discuss how the sensitivity of climate might be different if Earth's surface were 70% land and 30% ocean.
8. How do you think the behavior of the Daisyworld model might be different if the planet's sphericity were taken into account? Would it be more or less stable?
9. Program a time-dependent version of Daisyworld for the computer, but add an equation for the population of rabbits whose birth rate is proportional to the area covered by daisies. How does the approach to a steady state depend on the initial conditions and the parameters of the model? Add foxes.